Donor impurity states in wurtzite InGaN staggered quantum wells

Congxin Xia,[1,2,a)] Yalei Jia,[1] Shuyi Wei,[1] Yu Jia,[2,b)] and Harold N. Spector[3]
[1]*Department of Physics, Henan Normal University, Xinxiang 453007, China*
[2]*Center for Clean Energy and Quantun Structures and School of Physics and Engineering, Zhengzhou University, Zhengzhou 450052, China*
[3]*Department of Physics, Illinois Institute of Technology, Chicago, Illinois 60616, USA*

(Received 26 September 2011; accepted 30 October 2011; published online 18 November 2011)

Within the framework of the effective-mass approximation, donor impurity states in wurtzite (WZ) InGaN staggered quantum wells (QWs) are investigated theoretically. Numerical results show that the donor binding energy becomes insensitive to the variation of In composition y in the WZ $In_{0.2}Ga_{0.8}N/In_yGa_{1-y}N$ staggered QWs when $y > 0.125$ and for any impurity position. Moreover, for the impurity located at the right edge of the $In_yGa_{1-y}N$ well layer, the donor binding energy has a minimum and it is also insensible to the variation of well width in the staggered QWs when the well width $L > 3$ nm. © *2011 American Institute of Physics*. [doi:10.1063/1.3662848]

Recently, wide-band-gap wurtzite (WZ) GaN-based quantum wells (QWs) have attracted much attention due to potential device applications in electronics and optoelectronics devices.[1–3] High efficiency is the foremost importance in the devices application. However, there exits a strong built-in electric field caused by piezoelectric and spontaneous polarizations in WZ GaN-based QWs, which induces spatial separation between electron and hole wave functions and significantly reduces radiative recombination.[4,5] This obstacle is a major challenge for high efficiency optoelectronic devices based on conventional WZ GaN-based QWs. In order to overcome this shortcoming, different approaches have been proposed to reduce the built-in electric field effects, such as non-polar InGaN QWs,[6,7] type-II InGaN-GaNAs QWs,[8,9] AlGaN layer modulated InGaN QWs (Refs. 10 and 11), and InGaN staggered QWs.[12–15] One of these interesting methods is the fabrication of WZ InGaN staggered QWs, which is because the growth process is almost identical to the conventional structures, and the possibilities of crystal defects will not severely increase.[16] Moreover, the Light-emitting diode (LED) based on WZ InGaN staggered QWs shows a remarkable improvement in the photoluminescence intensity and output power.[17] It also offers an extra degree of freedom to tune the emission wavelength. Thus, electronics and optoelectronics devices based on WZ GaN-based staggered QWs have attracted an intensive attention as a promising candidate to overcome the built-in electric field effects. As is well known, impurity states play a very important role in the semiconductor optoelectronic devices.[18,19] Their presence can dramatically alters the performance of optoelectronic devices. More recently, the study of impurity in GaN-based quantum structures have attached much attention.[20,21] However, to our knowledge, there are few studies involved in impurity states in WZ InGaN staggered QWs.

In order to understand the donor impurity states in WZ InGaN staggered QWs, in this letter, we present the analysis of the donor binding energy of hydrogenic donor impurity in WZ InGaN staggered QWs following the theory of Ref. 22. The strength of the built-in electric field F caused by the spontaneous and piezoelectric polarizations in WZ $In_xGa_{1-x}N/In_yGa_{1-y}N$ staggered QWs is expressed as[23,24]

$$F = \begin{cases} 0, & |z| > L \\ \left| -\dfrac{P_{SP}^{InGan}(x) + P_{PZ}^{InGan}(x) - P_{SP}^{Gan}(x)}{\varepsilon_e^{InGan}(x)} \right|, & -L < z < 0 \\ \left| -\dfrac{P_{SP}^{InGan}(y) + P_{PZ}^{InGan}(y) - P_{SP}^{Gan}(y)}{\varepsilon_e^{InGan}(y)} \right|, & 0 < z < L \end{cases},$$

where $P_{SP}^{InGaN(GaN)}$ and P_{PZ}^{InGaN} are the spontaneous and piezoelectric polarizations of InGaN(GaN), respectively. ε_e^{InGaN} is electronic dielectric constant of material InGaN. As shown in Fig. 1, the built-in electric field modulates effectively band structure and electron wave function distribution in the WZ InGaN staggered QWs. All material parameters are taken from Refs. 24 and 25.

In order to understand the built-in electric field effects on the donor binding energy of impurity located at different positions in WZ InGaN staggered QWs. Fig. 2 shows that the

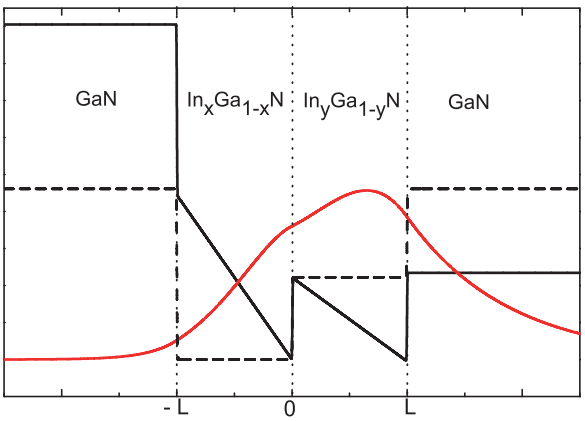

FIG. 1. (Color online) The conduction band potential profiles and the electron wave function in WZ InGaN staggered QWs. The black solid and dashed lines are for the band diagram of the staggered QWs with and without the built-in electric field. The red solid line for the electron function distribution.

a)Electronic mail: xiacongxin@henannu.edu.cn.
b)Electronic mail: jiayu@zzu.edu.cn.

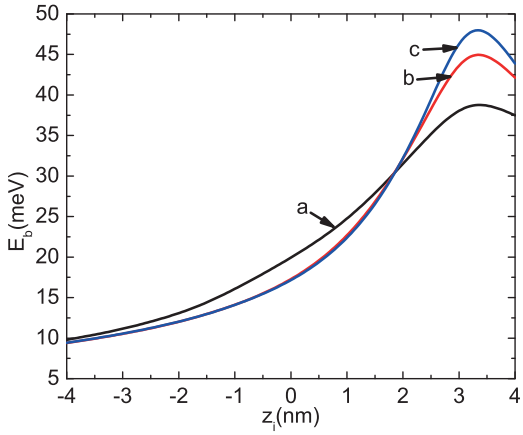

FIG. 2. (Color online) The ground-state donor binding energy E_b as a function of impurity position z_i in WZ $In_{0.2}Ga_{0.8}N/In_yGa_{1-y}N$ staggered QWs with well width L = 4 nm and for different In compositions y. The curves a, b, and c are for the In composition y = 0.05, 0.10, and 0.15, respectively.

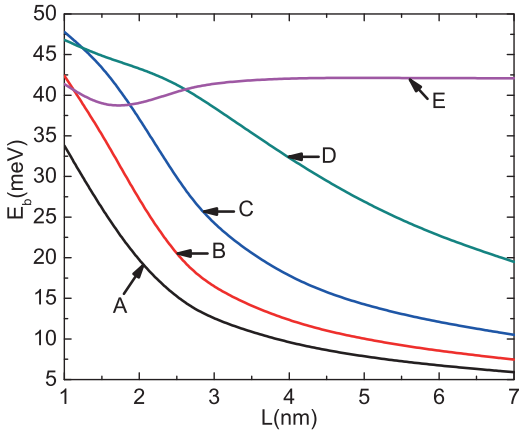

FIG. 4. (Color online) The ground-state donor binding energy E_b as a function of well width L in WZ $In_{0.2}Ga_{0.8}N/In_{0.1}Ga_{0.9}N$ staggered QWs for different impurity positions z_i. The curves A, B, C, D, and E are the same as in Fig. 3.

donor binding energy has a maximum with the variation of impurity position and the maximum value is located at the $In_yGa_{1-y}N$ well layer in the WZ $In_{0.2}G_{0.8}N/In_yGa_{1-y}N$ staggered QWs. This is because the built-in electric field pushes the electron distribution towards the $In_yGa_{1-y}N$ well layer. We can also find from Fig. 2 that for the impurity located at the $In_{0.2}G_{0.8}N$ well layer, the donor binding energy is larger for low In composition y; however, for the impurity located at the $In_yGa_{1-y}N$ well layer, it is larger for high In composition y. To make a clear understanding of the interesting phenomenon, in Fig. 3, the donor binding energy is investigated as a function of In composition y in WZ $In_{0.2}G_{0.8}N/In_yGa_{1-y}N$ staggered QWs.

It can be seen from Fig. 3 that, for the impurities located at $z_i = -L$, $-L/2$, and 0 (curves A, B, and C), the donor binding energy decreases first and then remains insensitive to the variation of In composition y when $y > 0.125$. This can be explained as follows. When In composition y increases, the energy gap of $In_yGa_{1-y}N$ well layer decreases and the electron is distributed towards the $In_yGa_{1-y}N$ well layer. However, when In composition $y > 0.125$, the electron is mostly confined inside the $In_yGa_{1-y}N$ well layer, the distance between the electron and the impurity located at the $In_{0.2}G_{0.8}N$ well layer is almost invariable. In addition, for the impurity located at $z_i = L/2$ (curve D), the donor binding energy increases to a maximum and then decreases slowly with the increase of In composition y, as expected. Moreover, Fig. 3 also shows that for the impurity located at $z_i = L$ (curve E), the donor binding energy increases rapidly first and then increases slowly when In composition $y > 0.125$. The reason is that when In composition y is low, the electron is mostly confined inside the $In_{0.2}G_{0.8}N$ well layer; when In composition y is high, the electron is confined inside the $In_yGa_{1-y}N$ well layer.

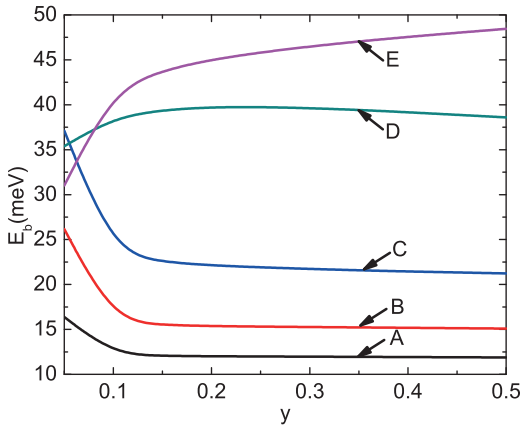

FIG. 3. (Color online) The ground-state donor binding energy E_b as a function of In composition y in WZ $In_{0.2}Ga_{0.8}N/In_yGa_{1-y}N$ staggered QWs with well widths L = 4 nm and for different impurity positions z_i. The curves A, B, C, D, and E are for the impurity position $z_i = -L$, $-L/2$, 0, L/2, and L, respectively.

In Fig. 4, the donor binding energy as a function of well width L in WZ $In_{0.2}G_{0.8}N/In_{0.1}Ga_{0.9}N$ staggered QWs for different impurity positions z_i is displayed. For the impurity located at $z_i = -L$, $-L/2$, and 0 (curves A, B, and C), the donor binding energy is decreased with the increase of well width L. This is because when well width L increases, the electron-impurity distance increases and Coulomb interaction decreases. For the impurity located at $z_i = L/2$ (curve D), the donor binding energy decreases slowly and then decreases rapidly when well width L increases. The reason is as follows. Though the electron distribution is shifted towards the right edge of the $In_{0.1}Ga_{0.9}N$ well layer which makes the donor binding energy decrease, the electron wave function distributed in the $In_{0.2}Ga_{0.8}N$ well layer is shifted towards the $In_{0.1}Ga_{0.9}N$ well layer. For their combined action, the donor binding energy of the impurity located at $z_i = L/2$ decreases slowly. When well width L is increased continually, the built-in electric field pushes the electron towards the right edge of the $In_{0.1}Ga_{0.9}N$ well layer, so the donor binding energy decreases rapidly. In particular, Fig. 4 also shows that for the impurity located at the right edge of the $In_{0.1}Ga_{0.9}N$ well layer (curve E), the donor binding energy is insensible to well width when the well width $L > 3$ nm, which is interesting to understand quantum size effects on electron and donor impurity states in WZ InGaN staggered QWs.

In summary, the donor binding energy of hydrogenic donor impurity in WZ $In_{0.2}Ga_{0.8}N/In_yGa_{1-y}N$ staggered QWs is studied. Our calculation shows that the donor binding energy has a maximum with the variation of impurity position and

the maximum value is at the $In_yGa_{1-y}N$ well layer. With the increases of In composition y, the donor binding energy decreases first and then remains insensitive to In composition y when $y > 0.125$ and for any impurity position. With the increase of the well width, the donor binding energy is decreased for the impurity located at $z_i = -L$, $-L/2$, 0, and $L/2$; while for the impurity located at the right edge of the $In_{0.1}Ga_{0.9}N$ well layer, when the well width $L > 3$ nm, the donor binding energy is insensible to the increasing well width. These results may be interesting and useful to understand the donor impurity states in WZ InGaN staggered QWs, which indicates that staggered QWs structure parameters can manipulate the electron and impurity properties in the WZ InGaN staggered QWs. Experimental studies for the hydrogenic donor impurity states in WZ InGaN staggered QWs are still lacking at present. We hope that our calculation can stimulate further investigations of the related physics, as well as device applications of group-III nitrides.

This work was supported by the National Natural Science Foundation of China under Grant No. 60906044.

[1]B. Gil, *Group III Nitride Semiconductor Compounds: Physics and Applications* (Clarendon, Oxford, 1998).
[2]S. Nakamura and S. F. Chichibu, *Introduction to Nitride Semiconductor Blue Lasers and Light Emitting Diodes* (Taylor and Francis, London, 2000).
[3]S. H. Han, D. Y. Lee, S. J. Lee, C. Y. Cho, M. K. Kwon, S. P. Lee, D. Y. Noh, D. J. Kim, Y. C. Kim, and S. J. Park, Appl. Phys. Lett. **94**, 231123 (2009).
[4]F. Bernardini, V. Fiorentini, and D. Vanderbilt, Phys. Rev. B **56**, R10024 (1997).
[5]P. Waltereit, O. Brandt, A. Trampert, H. T. Grahn, J. Menniger, M. Ramsteiner, M. Reiche, and K. H. Ploog, Nature **406**, 865 (2000).
[6]S. H. Park and S. L. Chuang, Phys. Rev. B **59**, 4725 (1999).
[7]K. M. Kelchner, R. M. Farrell, Y. D. Lin, P. S. Hsu, M. T. Hardy, F. Wu, D. A. Cohen, H. Ohta, J. S. Speck, S. Nakamura, and S. P. DenBaars, Appl. Phys. Express **3**, 092103 (2010).
[8]H. Zhao, R. Arif, and N. Tansu, J. Appl. Phys. **104**, 043104 (2008).
[9]I. Vurgaftman, J. R. Meyer, N. Tansu, and L. J. Mawst, Appl. Phys. Lett. **83**, 2742 (2003).
[10]H. Zhao, R. A. Arif, Y. K. Ee, and N. Tansu, IEEE J. Quantum Electron. **45**, 66 (2009).
[11]S. Park, J. Park, and E. Yoon, Appl. Phys. Lett. **90**, 023508 (2007).
[12]R. A. Arif, H. Zhao, Y. K. Ee, and N. Tansu, IEEE J. Quantum Electron. **44**, 573 (2008).
[13]C. T. Liao, M. C. Tsai, B. T. Liou, S. H. Yen, and Y. K. Kuo, J. Appl. Phys. **108**, 063107 (2010).
[14]H. Zhao, G. Liu, X. Li, G. Huang, J. D. Poplawsky, S. T. Penn, V. Dierolf, and N. Tansu, Appl. Phys. Lett. **95**, 061104 (2009).
[15]S. Park, D. Ahn, and J. Kim, Appl. Phys. Lett. **94**, 041109 (2009).
[16]M. Tsai, S. Yen, and Y. K. Kuo, Appl. Phys. A **104**, 621 (2011).
[17]R. Arif, Y. Ee, and N. Tansu, Appl. Phys. Lett. **91**, 091110 (2007).
[18]T. Ando, Y. Arakawa, K. Furuya, S. Komiyama, and H. Nakashima, *Mesoscopic Physics and Electronics* (Springer, Berlin, 1998).
[19]G. Bastard, Phys. Rev. B **24**, 4714 (1981).
[20]C. Xia, Z. Zeng, and S. Wei, J. Appl. Phys. **108**, 054307 (2010).
[21]L. Jiang, H. Wang, H. Wu, Q. Gong, and S. Feng, J. Appl. Phys. **105**, 053710 (2009).
[22]C. Xia, Z. Zeng, and S. Wei, J. Appl. Phys. **106**, 094301 (2009).
[23]C. Xia and S. Wei, Phys. Lett. A **161**, 359 (2006).
[24]F. Bernardini, V. Fiorentini, and D. Vanderbilt, Phys. Rev. Lett. **79**, 3958 (1997).
[25]J. J. Shi and Z. Z. Gan, J. Appl. Phys. **94**, 407 (2003).